Agricultural Water Management 318 (2025) 109704

Contents lists available at ScienceDirect

Agricultural Water Management

journal homepage: www.elsevier.com/locate/agwat

Year patterns of climate impact models' performance: Long-term simulation of rainfed spring wheat production using five crop models under various climate patterns

Funian Zhao [a,b,*], Qiang Zhang [a,**], Heling Wang [a,b], Kai Zhang [a,b]

[a] Key Laboratory of Arid Climatic Change and Disaster Reduction of Gansu Province/Key Laboratory of Arid Climate Change and Disaster Reduction of China Meteorological Administration/Institute of Arid Meteorology, China Meteorological Administration, Lanzhou 730020, China

[b] Dingxi Drought Meteorology and Ecological Environment Field Scientific Experimental Station of China Meteorological Administration, Dingxi 743000, China

ARTICLE INFO

Handling editor: Dr. Brent Clothier

Keywords:
Climatic pattern
Crop model
Drought
Model validation
Wheat

ABSTRACT

Crop models serve as powerful tools for investigating the interaction of crop traits, environmental fluctuations, and management practices. However, the calibration of these models relies heavily on experiments conducted under specific conditions or within particular years. The adaptability and efficacy of these calibrated models across different year patterns of climate remain uncertain. Our analysis aimed to evaluate the utility of these models across diverse climatic patterns and explore potential factors contributing to their performance variations. In this study, experiments were conducted in a semi-arid region characterized by significant climate variability, and data collection was undertaken to assess the performance of five distinct crop models (APSIM, AquaCrop, DSSAT, SSM-iCrop, WOFOST). The field experimental results indicated that year patterns of climate for rainfed spring wheat was jointly determined by soil water at planting and atmospheric moisture conditions during the growing season. After calibration, all five crop models effectively captured the growth, development, and yield formation of spring wheat. Notably, both simple and complex models exhibited similar performance in simulating the spring wheat growth and yield formation. However, the simulation results for spring wheat yield varied among the different year patterns of climate. Particularly in drier climate regimes, most models tended to overestimate spring wheat yields, with calculated relative root mean square errors exceeding 30 %. These findings suggested that calibrated models might not universally represent crop growth, development, and yield formation processes across all climatic patterns in regions characterized by substantial climate variability. In specific years, they were prone to either overestimating or underestimating crop yields. Furthermore, our study raised questions about the direct transferability of models to neighboring regions within the same climatic zone and application in future climatic scenarios. Without local climate-specific model calibration and with current climate-specific model calibration, the use of models might lead to inaccurate estimations of crop yields in other climatic area and future dryer climatic scenarios.

1. Introduction

Crop growth, development, and yield formation are the intricate outcomes of the interplay between environmental factors, inherent crop characteristics, and various management practices (Hajjarpoor et al., 2022; Teixeira et al., 2017). Understanding the intricate relationships among environment, genotype, and management interactions is crucial in agricultural research. Within this context, process-based crop modelling emerges as a pivotal tool to facilitate our understanding of these interactions (Hajjarpoor et al., 2022; Jones et al., 2017).

Numerous crop models have been developed over the years, each rooted in distinct mathematical frameworks and assumptions (Jin et al., 2016; Manschadi et al., 2020; Soltani and Sinclair, 2012). These variations can lead to different simulation results when applied to identical environmental settings, underscoring the importance of model selection in agricultural research. Meanwhile, as the climate evolves, crop

* Corresponding author at: Key Laboratory of Arid Climatic Change and Disaster Reduction of Gansu Province/Key Laboratory of Arid Climate Change and Disaster Reduction of China Meteorological Administration/Institute of Arid Meteorology, China Meteorological Administration, Lanzhou 730020, China.

** Corresponding author.

E-mail addresses: zhaofn@iamcma.cn (F. Zhao), zhangqiang@cma.gov.cn (Q. Zhang).

https://doi.org/10.1016/j.agwat.2025.109704
Received 30 December 2024; Received in revised form 11 July 2025; Accepted 26 July 2025

production is increasingly influenced by long-term shifts, increased interannual variability, and the occurrence of extreme climatic events (Otkin et al., 2018). These changing climate patterns introduce a layer of complexity to crop modeling, as models must accurately capture the dynamic interplay between crops and their evolving environments. Evaluating model performance needs an assessment across diverse climate patterns (Yu et al., 2014). In practice, during parameter estimation, models frequently face difficulties in comprehensively representing the entire range of climatic conditions (White et al., 2025). Most experiments for model improvement are conducted under close to optimum conditions, possibly limiting their performance under varying environmental conditions (Wallach and Thorburn, 2017). However, previous research findings have been contradictory. In some researches, crop models have been found to overestimate yields during periods of extreme wetness and underestimate them during droughts (Balwinder-Singh et al., 2011; Yu et al., 2014). Paradoxically, some studies suggest that crop models might overestimate yields during dry periods (Fletcher et al., 2020; Hao et al., 2021; White et al., 2025), adding to the complexity of model evaluation.

Climate transitional regions like semi-arid areas exhibit substantial interannual variability in climatic conditions due to the influence of precipitation variability (Zhao et al., 2022, 2024). The interannual variability of climate is often much greater than the rate of long-term climate change (Zhang et al., 2019). This presents favorable environmental conditions for model assessment, making it highly suitable for studying the applicability of crop models and assessing their simulation performance in the context of climate change. While comparative studies of models across geographical regions can allow to analyze such differences, variations in factors like soil, crop varieties, and management practices introduce additional complexities (Ramirez-Villegas et al., 2017). Therefore, the choice to focus on a single site within a semi-arid region for a multi-year comparative analysis of crop model applications under different annual climatic conditions is advantageous.

The complex interactions between crops and the environment, along with possible differences in model performance, highlight the need for a systematic model evaluation, which may allow us to gain invaluable insights into their robustness and limitations (Kleinwechter et al., 2016; Manschadi et al., 2020). Therefore, the primary goals of this study were: a) to systematically analyze crop development and growth responses to environmental conditions of rainfed spring wheat (*Triticum aestivum* L.), and b) to use the experimental data to evaluate five crop models on their capability to capture the interannual variability of crop development and growth of biomass and gran yield under various climate patterns.

2. Materials and methods

2.1. Study area

This research was carried out in the Western Loess Plateau, located in the Northwest of China (Fig. 1). The area is located within a climatic transition zone and agro-pastoral ecotone. It is classified as a semi-arid area, situated between arid and semi-humid regions (Zhao et al., 2018). The region experiences a total mean annual precipitation ranging from 350 to 500 mm. Notably, 60 % of the annual rainfall is concentrated from July to September, with only approximately 30 % occurring from March to June, coinciding with the spring wheat growing season (Fig. 2). The soil in this area is characterized as loessial, with clay content ranging from 33.1 % to 42.2 %, classified it as sandy loam. The soil depth averages between 40 and 60 m, and the soil organic matter (SOM) content varies from 0.4 % to 1.4 %.

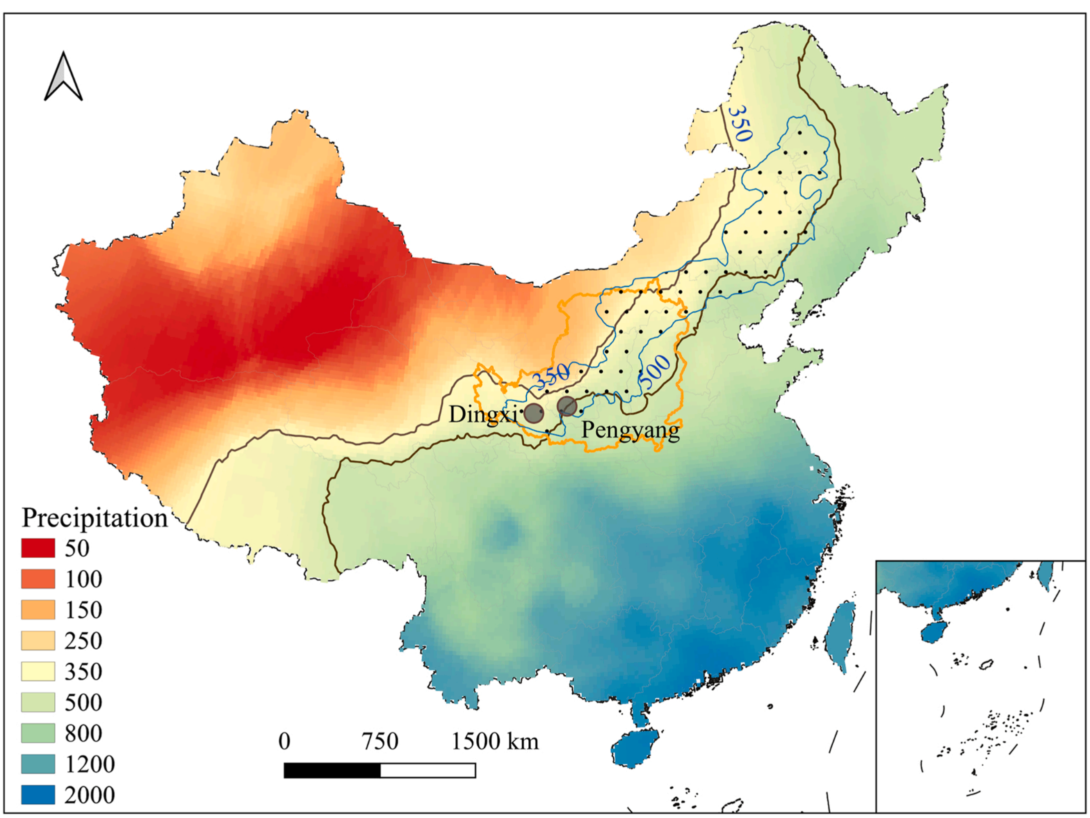

Fig. 1. Geographical locations and average annual precipitation over a 32-year period from 1987 to 2018. The brown solid lines represent the isohyets for precipitation amounts of 350 mm and 500 mm, respectively. The average annual precipitation data from 1987 to 2018 were collected from a total of 2382 ground-monitoring meteorological stations across China. The area outlined with solid yellow lines indicates the Loess Plateau, while the area marked with solid blue lines and dots represents the agro-pastoral ecotone.

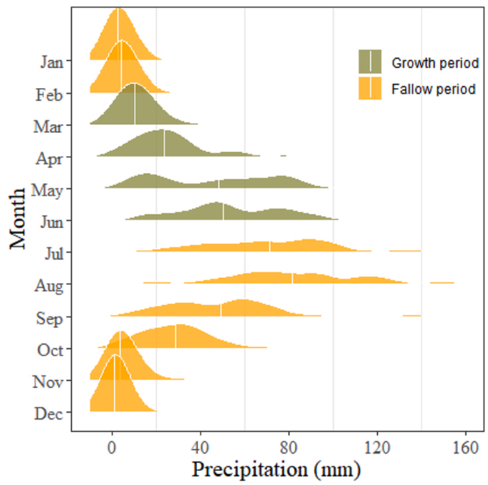

Fig. 2. Precipitation distripution in Dingxi, Northwest of China.

2.2. Experimental data collection

Two main data categories were used as the information source for parameterization and assessment of different wheat growth models. The first dataset originates from field experiments, encompassing the following:

1) The first, a long term experiment conducted at the Dingxi Agricultural Meteorological Experiment Station (104.62°E, 35.58°N, 1896.7 m.a.s.l.), between 1987 and 2018. The experiment consisted of a single rain-fed treatment with four replications. Spring wheat was sown in mid-to-late March each year, preceded by the application of an (put the range of basal fert) basal fertilizer, including farmyard manure and nitrogen fertilizer (Refer to Table S1 for planting and fertilization details). Measured variables included development days, plant density at jointing, leaf area index (LAI) at flower period (which defined the maximum LAI during growing season), aboveground biomass at maturity, and final grain yield.
2) The second experiment consisted of planting date experiments carried out at the Dingxi Agricultural Meteorological Experiment Station in 2010. The selected spring wheat variety was Dingxi New 24, grown under rain-fed conditions. This experiment involved four planting periods on March 8th, 18th, 28th, and April 7th, each with three replications. Adequate basal fertilizer, including 15,000 kg ha^{-1} of farmyard manure and 150 kg ha^{-1} of urea, was applied during planting. Measured variables included development days, aboveground biomass at maturity, and final yield.
3) The third and last field experiment, was an irrigation experiment conducted in 2016 at the Pengyang Dryland Agricultural Experiment Station (106.39°E, 35.55°N, 1782 m.a.s.l). Selected spring wheat cultivar was Dingxi 40, sown on March 25th. Six water treatments were implemented, each with three replications. Treatments included different irrigation levels (30, 60, 90, 150 mm), a completely rain-sheltered treatment with no irrigation and a control (rain-fed conditions). Irrigation treatments were applied in three stages during the growth period, with each stage receiving one-third of the total water amount on May 4th (6-leaf stage), May 22nd (jointing stage), and June 15th (grain filling stage), respectively. Developmental stages of spring wheat were recorded during the experiment, and aboveground biomass at maturity and final grain yield were determined after harvest. Adequate fertilizer supply was ensured by applying farmyard manure at 30,000 kg ha^{-1} and urea at 225 kg ha^{-1} before planting. For more detailed procedures and experimental specifics regarding the long-term field experiment and irrigation experiment, please refer to Zhao et al. (2022). Additionally, for a comprehensive introduction to the planting dates experiment, please refer to Zhang et al. (2012).

The second dataset was obtained from published literature on spring wheat experiments conducted in the semi-arid region at the Western Loess Plateau. These data were gathered by searching the China National Knowledge Infrastructure (CNKI) database and Web of Science database using keywords such as "spring wheat," "semi-arid region," "Dingxi," and "Western Loess Plateau" from 1995 to 2018. Information related to spring wheat planting, treatment methods, growth periods and aboveground biomass data was extracted directly from the literature text or tables obtained from the search. In some cases, data was extracted from literature figures using GetData graph digitizing software (http://getdata-graph-digitizer.com). It was important to note that the experiments described in the literature encompassed a variety of treatments involving different water, fertilizer, and coverage methods. However, for analysis purposes, only the results from experiments with varying water levels, medium and high-level fertilizer treatments, and traditional tillage methods were selected, for more details referred to Zhao et al. (2019). The literature and experimental information are presented in Table S2.

All three field experiments were equipped with ground meteorological observation stations located within 100 m. Meteorological parameters for the respective experimental years, including daily sunshine hours, maximum and minimum temperatures, relative humidity, wind speed, and precipitation, were obtained through the ground meteorological observation stations. Daily solar radiation was estimated from sunshine hours, latitude and longitude of the observation site, and the day of the year based on Angstrom equation (Allen et al., 1998). Vapor pressure deficit was derived from daily average temperature and relative humidity. Reference evapotranspiration was computed using the Penman-Monteith formula. For detailed calculation procedures, please refer to the FAO-56 manual documentation (Allen et al., 1998). All meteorological variables discussed in the literature were collected and analyzed using data from the Dingxi Agricultural Meteorological Experimental Station, which was situated within the Dingxi region as mentioned. Meanwhile, we introduced the concept of atmospheric moisture conditions, defined as the difference between reference evapotranspiration and precipitation during the spring wheat growing season, to better quantify the growth environment for spring wheat. Additionally, in each experiment, soil water content was determined using gravimetric sampling at 10 cm increments from the surface to a depth of 100 cm for each experiment. These gravimetric measurements were converted to volumetric water content using the bulk density of each corresponding soil layer. The soil water content used in this study was the total water content in soil from surface layer to 100 cm.

2.3. Crop models description

Among the five crop models, two simpler models were tested: Aquacrop (Steduto et al., 2009) and SSM-iCrop (Soltani et al., 2020; Soltani and Sinclair, 2012). The three more complex models were APSIM (Keating et al., 2003), DSSAT (Jones et al., 2003) and WOFOST (de Wit et al., 2019).

AquaCrop is a semi-empirical, crop-water productivity model that primarily focuses on water-limited conditions (Steduto et al., 2009). It is a water-driven crop growth model designed for agricultural planning and scenario analysis. AquaCrop simplifies crop growth modeling by emphasizing water stress and the impact on crop development and yield. It performs daily water balance computations by accounting for all key hydrological processes: infiltration, surface runoff, deep percolation, soil evaporation, and plant transpiration, along with tracking soil moisture dynamics. The simplicity of AquaCrop makes it an efficient tool for regions with limited data, and its ability to quantify water productivity is particularly useful for optimizing irrigation practices and resource management.

SSM-iCrop is designed as a simplified, user-friendly model suitable for resource-constrained environments (Sinclair, 1986; Soltani et al., 2020). The model can simulate three yield levels: the crop potential yield limited by light and temperature, the rainfed yield limited by light, temperature, and water, and the attainable yield limited by light, temperature, water, and fertilizer. In this model, the impact of drought on crop dry matter accumulation, leaf growth, and phenology is determined by stress coefficients calculated through piecewise functions. These functions are based on threshold responses of crop leaf gas exchange, leaf growth, and phenological development to soil available water content during drought conditions. It simulates crop growth, water balance, and nutrient dynamics with minimal input data requirements (Soltani and Sinclair, 2012). It aims to promote agricultural decision-making in regions with limited resources. The ease of use and low data demands of SSM-iCrop make it accessible for farmers and researchers in areas with limited infrastructure. It prioritizes simplicity and practicality while still providing valuable insights.

APSIM is a process-based model that is used to simulate various aspects of crop production, including soil processes, water balance, crop growth, and management practices (Keating et al., 2003). It offers a wide range of options for representing complex farming systems and diverse crops. The model integrates specific soil, climate, and management input data. Simulated plant and soil processes include photosynthesis and carbon allocation, phenological development, root growth and water uptake, nutrient cycling, soil organic matter decomposition, evaporation and transpiration, tillage effects, residue decomposition, and interactions between crops and the environment under varying climatic and management conditions. The strength of this model lies in its flexibility, allowing researchers to tailor the model to specific cropping systems which makes it suitable for a broad spectrum of research applications.

DSSAT is a comprehensive suite of crop models that encompasses a wide range of crops, soil types, and management practices (Jones et al., 2003). It integrates weather, soil, and crop information to simulate crop growth, yield, and nutrient dynamics. DSSAT is widely recognized and used for decision support and research purposes. The strength of DSSAT lies in its versatility and extensive database of crop parameters, which allows it to model a wide array of cropping systems globally. Its ability to simulate diverse crops under varying conditions makes it a valuable research tool.

WOFOST is a widely-applied crop growth model known for its ability to estimate crop yields based on weather, soil, and management data (de Wit et al., 2019). It has been used extensively in various regions and for a wide range of crops. The adaptability of WOFOST to different climates and crops, along with its historical use in international research, make it a valuable tool for global agricultural assessments. Its simplicity in terms of input requirements and reliability in yield predictions contribute to its popularity.

Each of these crop models offers unique characteristics catering to specific research needs and environmental conditions. Researchers choose a model based on the complexity of the study system, data availability, and the specific research objectives (Jin et al., 2016; Soltani and Sinclair, 2015), with APSIM and DSSAT providing flexibility (Soltani and Sinclair, 2015), AquaCrop focusing on water stress (Steduto et al., 2009), SSM-iCrop simplifying modeling for resource-limited areas, and WOFOST's adaptability to diverse regions and crops (de Wit et al., 2019). The models with respect to the approaches they used to simulate different crop processes were summarized in Table 1 (Palosuo et al., 2011; Soltani and Sinclair, 2015).

Table 1
Simulating crop processes in the five evaluated crop models.

Component	APSIM	AQUACROP	DSSAT	SSM-iCrop	WOFOST
Phenology[a]	T/V/P/W	T/P	T/V/P	T/V/P/W	T/V/P
Water relation[b]	D	S	D	S	D
Leaf area changes[c]	D	S	D	S	S
Dry matter production[d]	RUE/TE	TE	RUE	RUE	P-R
Dry matter partitioning[e]	PC-D	PC-S	PC-D	PC-S	PC-S
Yield formation[f]	Part/GNA/DHI	HI	GNA	DHI	Part
Plant nitrogen budget[g]	D	-	D	S	-

[a] T, temperature; V, vernalization; P, photoperiod; W, water stress.
[b] D, detailed approach including root growth and water absorption; S, simple approach including linear increase in root depth.
[c] D, detailed approach from individual leaf area; S, simple approach from whole plant leaf area or allometric relationships.
[d] RUE, radiation use efficiency approach; TE, relation between mass production and transpiration; P-R = Detailed (explanatory) Gross photosynthesis – respiration.
[e] PC-D, detailed approach partitioning coefficients and more organs; PC-S, simple approach partitioning coefficients and fewer organ.
[f] Part, approach with partitioning during reproductive stages; GNA, approach with grain number; DHI, approach of linear increase in harvest index; HI, approach with harvest index modified by water stress.
[g] D, detailed approach with concentration curves for different organs over the growth period; S, simple approach with fixed concentrations in green and senesced organs.

2.4. Models parameterization and evaluation

APSIM 7.10 (run via visualization platforms), DSSAT 4.7 (run via visualization platforms), PyWOFOST (run in Python), AquaCrop-OSPy (run in Python), and SSM-Wheat (run in Excel using VBA) were the versions of the five crop models used for simulation of spring wheat growth and yield formation in the current study. For Models parameterization, we adjusted only a limited set of parameters within each model using the methods described by Soltani and Sinclair (2015).

APSIM operates under the default assumption that most users will not need to change its core model parameters. Consequently, detailed guidance on calibrating the model for new crop varieties is not included in its documentation. However, the system does allow modifications to predefined parameter values when necessary. The framework organizes crop parameters into two broad classifications: the majority are fixed values shared across all varieties, while a smaller set can be fine-tuned for specific cultivars. Ten key parameters are commonly used by APSIM to characterize cultivar properties (Table 2). Adjusting these parameters allows for the creation of new cultivars. These adjustable parameters mainly influence developmental timing (phenology) and yield-related traits, including grain properties, weight, and shifts in harvest index over time.

In DSSAT, crop parameters are further subdivided into three categories. The first category, known as the 'species' part, remain uniform for all cultivars within a given crop type. The second category, the 'ecotype' part, groups 32 parameters that are treated as stable across related cultivars. The third category relates to 'cultivar' parameters, consisting of seven parameters associated with phenology and yield formation (Table 2).

In the case of AquaCrop, WOFOST and SSM-iCrop, parameters are not explicitly categorized. To simulate different cultivars in our study, we needed to estimate specific parameters for the three models. The other parameters remained fixed across all cultivars. A list of these cultivar-specific parameters for the evaluated models could be found in Table 2. The basic information on soil properties was shown in Table 3.

In this study, data collected from reference, different planting date experiment from the Dingxi Agricultural Meteorological Experimental Station, and irrigation in different growth stage experiment from the Pengyang Dryland Farming Experimental Station were used for the parameterization and calibration of the models. Since most of the data

Table 2
List of cultivar parameters in APSIM, AquaCrop, DSSAT, Wofost and SSM-iCrop.

Parameter	Value
APSIM	
Thermal time from start of grain filling to maturity (°C)	580
Grain number per spike	30
Filling rate (mg (grain d)$^{-1}$)	2.3
Tiller weight (g)	1.22
Individual plant weight (g)	4
Stem length (mm)	1000
Vernalization sensitivity	1
Photoperiod sensitivity	2.0
Potential grain filling rate (g grain^{-1} d^{-1})	0.001
Maximum grain size (g)	0.045
AquaCrop	
GDDays: Thermal time from sowing to emergence (°C)	150
GDDays: Thermal time from sowing to maximum rooting depth (°C)	924
GDDays: Thermal time from sowing to start senescence (°C)	1310
GDDays: Thermal time from sowing to maturity (length of crop cycle) (°C)	1650
Length of the flowering stage (growing degree days) (°C)	150
Reference Harvest Index (HIo) (%)	0.42
Maximum effective rooting depth (m)	1.0
Maximum canopy cover (%)	0.96
Standardized water production efficiency (g m^{-2})	15
Transpiration coefficient of crops under complete canopy cover without senescence	1.1
DSSAT	
Days at optimum vernalizing temperature required to complete vernalization (d)	6.1
Percentage reduction in development rate in a photoperiod 10 h shorter than the threshold relative to that at the threshold (%)	38.3
Grain filling (excluding lag phase duration) (°C)	449.2
Kernel number per unit canopy weight at anthesis (simple g^{-1})	15.6
Standard kernel size under optimum conditions (mg)	20.43
Standard, non-stressed dry weight (total, including grain) of a single tiller at maturity (g)	1.032
Interval between successive leaf tip appearances (°C)	98.5
Wofost	
Temperature sum from sowing to emergence (°C)	150
Temperature sum from emergence to anthesis (°C)	870
Temperature sum from anthesis to maturity (°C)	590
Initial total crop dry weight (kg ha−1)	15
Leaf area index at emergence	0.104
Maximum relative increase in LAI	0.0071
Life span of leaves growing at 35 Celsius (d)	25
Efficiency of conversion into leaves (kg kg^{-1})	0.72
Efficiency of conversion into storage organization (kg kg^{-1})	0.74
Efficiency of conversion into stems (kg kg−1)	0.69
Maximum rooting depth (cm)	100
Maximum daily increase in rooting depth (cm d^{-1})	2
Maximum. leaf CO2 assimiliation rate at anthesis (kg ha^{-1} hr^{-1})	35
SSM-iCrop	
Vernalization sensitivity coefficient	0.00089
Photoperiod sensitivity coefficient	0.000147
Temperature unit from sowing to emergence (°C)	150
Temperature unit from sowing to maturity (°C)	1650
Temperature unit from sowing to beginning seed growth (°C)	1020
Maximum leaf area index	3.5
Maximum harvest index	0.42
Fraction crop mass at beginning seed growth which is translocateble to grains (g g^{-1})	0.12
FTSW threshold when dry matter production starts to decline	0.4
FTSW threshold when leaf area development starts to decline	0.5
Maximum effective depth of water extraction from soil by roots (mm)	1000

collected from the literature lack information of soil water content at planting, which is crucial for the growth, development, and yield formation of spring wheat, we categorized the data used for model calibration into different purposes. First, we used experimental data from different planting dates and literature-collected data to calculate the accumulated temperature during various growth stages of spring wheat (Fig. 3), calibrating the accumulated temperature-related parameters in each model. Second, we employed experimental data from different water treatments at the Pengyang Station to calibrate biomass and yield. Additionally, one year of complete crop growth data (aboveground biomass) from the collected literature was also used to calibrate parameters related to biomass and yield. The parameter calibration strategy in this study aimed to derive a single set of crop parameters that reflect multi-year conditions, effectively capturing the impact of varying climatic and environmental conditions (light, temperature, water, and soil water content at planting) on crop growth, development, and yield formation. Hence, spring wheat was represented by a fixed cultivar across the entire period, each model required only one parameter set.

Parameters governing spring wheat growth and development were refined through literature review, experimental observations, and model calibration. Furthermore, previous researchers have conducted simulation studies using APSIM (Nie et al., 2018) and DSSAT (Li et al., 2021) for spring wheat growth, development, and yield formation in the study region. In this research, we referred to and revised the model parameter values they used.

To evaluate if breeding effects had enhanced yield capacity over time in long-term studies conducted in Dingxi from 1987 to 2018, a simple linear regression analysis was performed, correlating spring wheat yield with the year based on data from long-term observational experiments. However, the results did not indicate any significant changes in spring wheat yield potential over the years ($p > 0.1$ in the linear model). Therefore, no adjustments were made to the yield data to account for an increasing yield trend due to genetic improvements when assessing crop models' performance in this region. Given this, our study would not attribute annual changes in spring wheat yield to varietal variations. Instead, we attributed them entirely to changes in climate conditions. Additionally, considering that the spring wheat varieties used in the experimental data were all medium to late-maturing varieties, we used a single variety in the spring wheat simulation process. This approach eliminated differences in simulation results caused by variations in crop genetic parameters.

Long-term observational experiments at the Dingxi Agricultural Meteorological Experimental Station were employed for model validation. Model evaluation metrics included the root mean square error (RMSE), relative root mean square error (RRMSE), index of agreement (d), and coefficient of determination (R^2), among others. Specific calculation procedures for these statistical metrics could be found in Correndo et al. (2022).

2.5. Statistical analysis

In order to determine the key climatic factors affecting spring wheat yield, a two-step methodology was employed based on data collected from long-term field experiment in Ding xi. Firstly, we posited that climate played a decisive role in determining yield, and consequently, we grouped soil water content at planting, growing season precipitation, temperature, radiation, vapor pressure deficit, reference evapotranspiration, and atmospheric moisture condition into eight distinct clusters. Subsequently, we conducted tests to ascertain whether the spring wheat yield distribution within each cluster significantly differed from that of any other cluster (Yu et al., 2014). This cluster analysis was deployed to uncover agro-climatological year patterns for spring wheat in Dingxi. The K-means clustering method was implemented using R software (R Development Core Team, 2024). To classify these clusters, we considered the spring wheat yield alongside the corresponding environmental variables such as soil water content at planting, growing season precipitation, temperature, radiation, vapor pressure deficit, reference evapotranspiration, and atmospheric moisture condition. These patterns were then categorized into groups, distinguishing between those that exhibited statistical significance and those that did not. The Kolmogorov-Smirnov (K-S) test was applied to ensure the statistically significant differentiation of each cluster from the others. In instances where no significant differences were detected, two patterns were merged into a single category. This iterative process was repeated until a significant difference was established between all patterns.

Table 3
Soil properties of experimental sites at Dingxi at depths of 0–100 cm.

Parameters	Soil depth (mm)					
	0–50	50–100	100–200	200–400	400–600	600–1000
Bulk density (g cm^{-3})	1.29	1.23	1.33	1.2	1.14	1.14
Air-dried moisture (mm mm^{-1})	0.01	0.01	0.05	0.07	0.09	0.10
Field capacity (mm mm^{-1})	0.27	0.27	0.27	0.27	0.26	0.26
Saturated moisture (mm mm^{-1})	0.46	0.49	0.45	0.5	0.52	0.52
Wilting coefficient (mm mm^{-1})	0.09	0.09	0.09	0.09	0.09	0.11
Soil water conductivity (mm h^{-1})	0.6	0.6	0.6	0.6	0.6	0.6

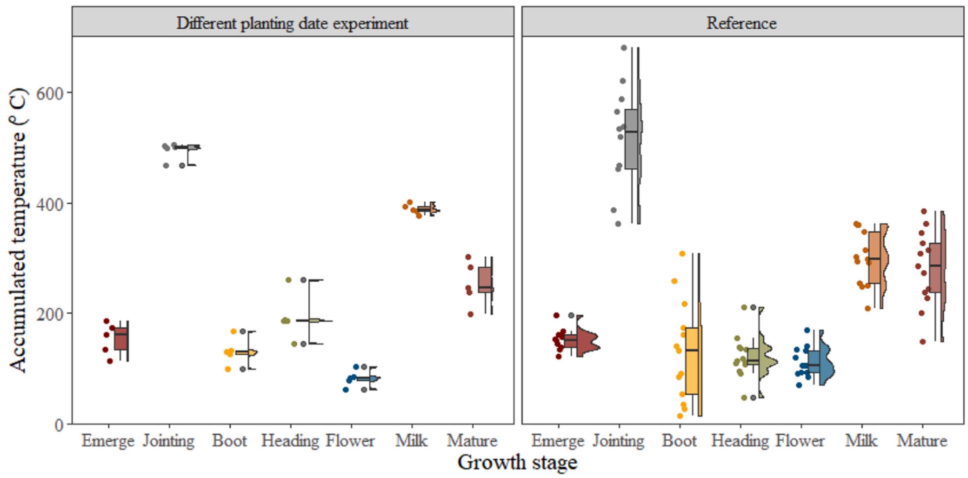

Fig. 3. Data of accumulated temperature during different growth stage for spring wheat collected from different planting date experiment and reference in Dingxi (Table S2).

With the software of R, linear regression and correlation analysis were employed to correlate with simulated value and observed value for spring wheat yield and aboveground. Meanwhile, we employed a random forest model named "randomForest" package in R to analyze the response relationship between normalized yield and environmental factors. Furthermore, the "varImp" function within "caret" package in the R estimated the relative importance of environmental factors in determining spring wheat yield.

3. Results

3.1. Year patterns of climate for spring wheat

3.1.1. Relations of environmental factors and spring wheat yield

The normalized yield of spring wheat increased with higher growing season precipitation, greater soil water content at planting, and increased May precipitation. In contrast, it declined with rising maximum temperatures in May, elevated atmospheric moisture condition during the growing season, higher average temperatures in June, and increased reference evapotranspiration in May (Fig. S1). Analysis using two distinct machine learning approaches consistently identified growing season precipitation, soil water at planting, maximum temperature in May, vapor pressure deficit in May, and growing season atmospheric moisture conditions as the most influential environmental factors affecting spring wheat yield (Fig. S2).

Further analysis of the correlations between spring wheat yield and key environmental factors revealed a strong positive association between growing season precipitation and yield (Fig. S3), with a correlation coefficient of 0.54. Soil water content at planting also showed a significant positive correlation with yield ($r = 0.50$). In contrast, growing season atmospheric moisture conditions were negatively correlated with yield, exhibiting a stronger magnitude than other variables. Additionally, maximum temperature, precipitation, vapor pressure deficit, and atmospheric moisture conditions in May all showed statistically significant correlations with spring wheat yield.

Moreover, our analysis revealed that soil water content at planting was strongly correlated with spring wheat tiller density at the jointing stage (Fig. 4). Tiller density at the jointing stage, in turn, was significantly correlated with the maximum LAI during the growing season, which was further correlated with aboveground biomass. Aboveground biomass exhibited a strong and significant correlation with final yield (Fig. 4). Notably, the correlation between soil water at planting and the maximum LAI during the growing season was particularly high, with a statistically significant correlation coefficient of 0.74 (figure was not shown).

3.1.2. Year patterns of climate for spring wheat

Cluster analysis revealed that inter-annual variations in spring wheat yield within the study area could be classified into five distinct categories (Fig. S4, Table S3). Across these categories (from A to E), growing season vapor pressure deficit, reference evapotranspiration, and atmospheric moisture conditions exhibited an increasing trend, while soil water at planting, growing season precipitation, maximum LAI, and aboveground biomass showed a corresponding decreasing trend. Based on the outcomes of the correlation analysis, we propose that these climatic yield patterns could be effectively characterized using two key indicators, soil water content at planting and growing season atmospheric moisture conditions (Fig. 5).

Specifically, climatic patterns of years for spring wheat yields were classified into the following categories: A (high soil water at planting and relatively wet growing season), B (high soil water at planting and relatively dry growing season), C (moderate soil water at planting and moderate drying during the growing season), D (moderate soil water at planting and relatively dry growing season), and E (low soil water at planting and relatively dry growing season) (Fig. 6). We suggested that higher soil water content at planting supported improved spring wheat

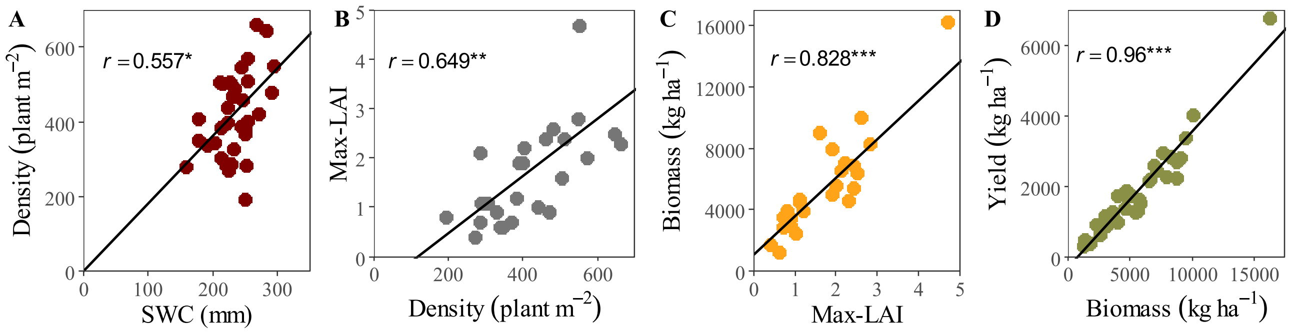

Fig. 4. Response of plant density at jointing (A), maximum leaf area index (B), aboveground biomass (C) and yield (D) to soil water content at planting (SWC), plant density at jointing, maximum leaf area index (Max-LAI) and above ground biomass at maturity for rainfed spring wheat, respectively, from 1987 to 2018 in Dingxi.

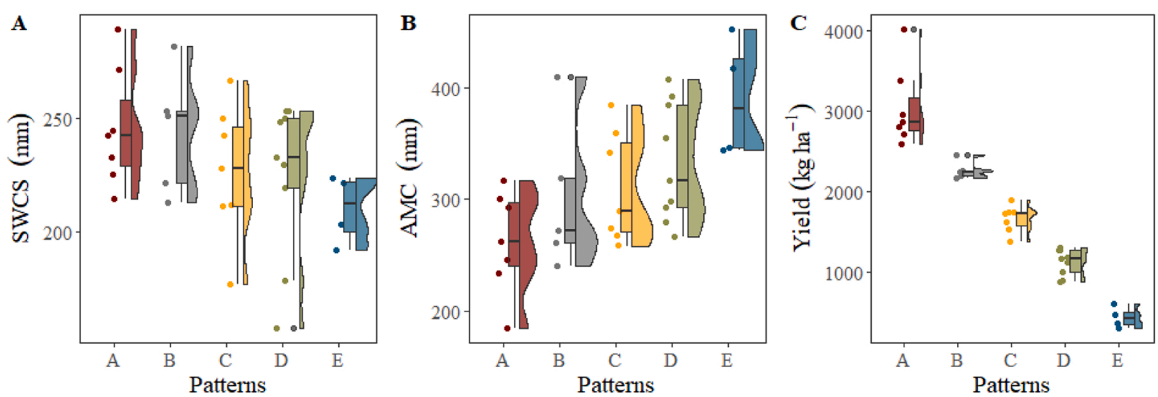

Fig. 5. Year patterns of climate for spring wheat at Dingxi. Thick black line is the median. Horizontal bars and upper and lower edges of boxes indicates 10, 25, 75, and 90 percentiles. SWCS indicates soil water content at planting. AMC indicates atmospheric moisture conditions (difference between growing season reference evapotranspiration and precipitation). Yield indicates spring wheat final grain yield.

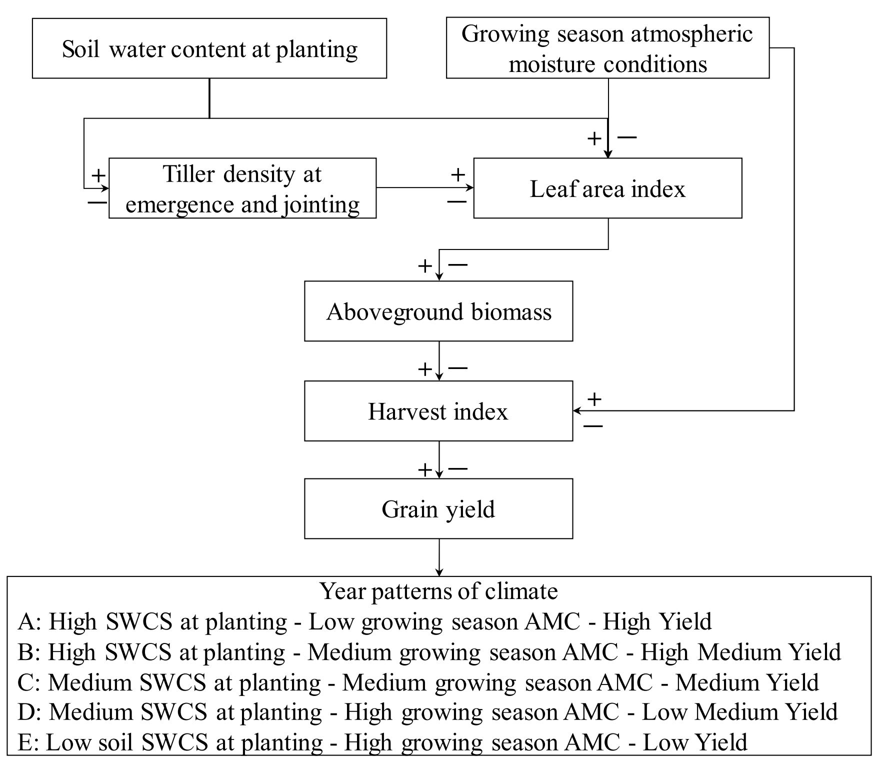

Fig. 6. The scheme showing the effects of soil water content at planting (SWCS) and growing season atmospheric moisture conditions (AMC) on tiller density, leaf area index, crop growth, harvest index and final grain yield. '+ ' is positive feedback and '–' negative.

emergence and promoted greater LAI and biomass accumulation during the vegetative growth stage. Furthermore, decreased atmospheric moisture conditions during the growing season contributed to a higher harvest index and enhanced grain yield. In contrast, years characterized by limited soil water at planting and drier atmospheric moisture conditions during the growing season were associated with reduced spring wheat yields.

3.2. Spring wheat production simulation

3.2.1. Models parameterization and evaluation

Through iterative calibration of model parameters using data from experiments with varying planting dates, irrigation treatments, and literature-derived information, we found that all five crop models effectively simulated the dynamics of aboveground biomass accumulation in spring wheat across its growth stages (Fig. 7). Among them, the APSIM and SSM-iCrop models demonstrated superior performance, exhibiting relatively low RMSE values and RRMSE values below 20 %. In contrast, the DSSAT model showed comparatively higher RMSE and RRMSE values. Notably, the ensemble simulation combining all five models yielded the most accurate results, with an RMSE of 10.8 g m^{-2} and an RRMSE of 8.2 %.

All five models were able to accurately simulate the aboveground biomass at maturity and final yield of spring wheat under different irrigation treatments throughout the growing season (Fig. 8). The discrepancies between simulated and observed values for both biomass and yield generally fell within a ± 30 % range. Among the models, APSIM demonstrated the best performance, with the lowest RMSE and RRMSE, as well as the highest *d* and R^2. In contrast, the DSSAT model showed the poorest performance, yielding the highest RMSE and RRMSE values and the lowest d and R^2 values. The simpler SSM-iCrop model also produced reliable simulations, with RRMSE values below 30 % and d values exceeding 0.8, indicating that even relatively simple models can achieve a reasonable level of accuracy compared to more complex models. Furthermore, ensemble averaging of biomass and yield simulations from all five models resulted in improved overall accuracy, with RMSE values of 748.7 kg ha^{-1} and 318.8 kg ha^{-1}, RRMSE values of 10.7 % and 12.6 %, and high agreement metrics ($d = 0.969$ and 0.963; $R^2 = 0.953$ and 0.989).

Using long-term observational data from the Dingxi Agricultural Meteorological Experimental Station to validate the simulation results of five crop models (Fig. 9), we observed a notable decline in simulation accuracy. Among the five models, the minimum RMSE for aboveground biomass at maturity was 1443 kg ha^{-1} (APSIM), while the maximum reached 2454 kg ha^{-1} (DSSAT). The RRMSE ranged from 26.6 % (SSM-iCrop) to 35.0 % (DSSAT), and the *d* varied between 0.632 (DSSAT) and 0.798 (WOFOST). For simulated final grain yield, RMSE values ranged from 486.8 kg ha^{-1} (SSM-iCrop) to 626.8 kg ha^{-1} (DSSAT), with corresponding RRMSE values between 25.1 % (AquaCrop) and 36.7 % (DSSAT). The index of agreement for yield simulations ranged from 0.751 (DSSAT) to 0.820 (AquaCrop). When applying a multi-model ensemble approach that combined outputs from all five models, the RMSE and RRMSE for biomass and yield were substantially reduced, 1279.9 kg ha^{-1} (22.6 %) for biomass and 385.9 kg ha^{-1} (20.8 %) for yield. The index of agreement also improved, reaching 0.833 for biomass and 0.887 for yield. Compared to individual models, the ensemble approach yielded lower RMSE and RRMSE values and higher agreement indices, suggesting that a multi-model ensemble provides a more accurate and robust simulation of spring wheat biomass and yield.

3.2.2. Simulation of spring wheat production under different year patterns of climate

An analysis of spring wheat yield simulations from five different models under varying climate patterns revealed distinct model performance trends (Fig. 10). Under climate patterns D and E, all models, except WOFOST, as well as the ensemble of all five models, tended to

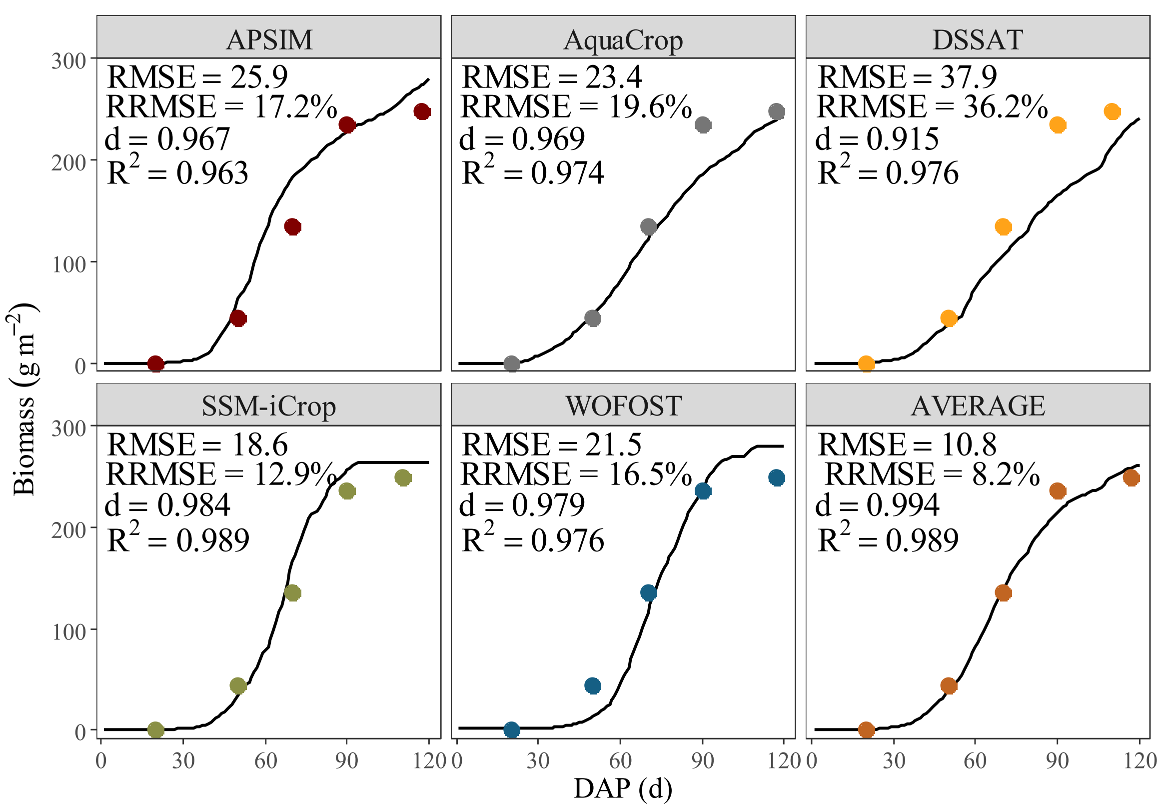

Fig. 7. Change of observed aboveground biomass observed (Li et al., 2004) and simulated aboveground biomass by different crop models. AVERAGE indicates the ensemble value of the five different models.

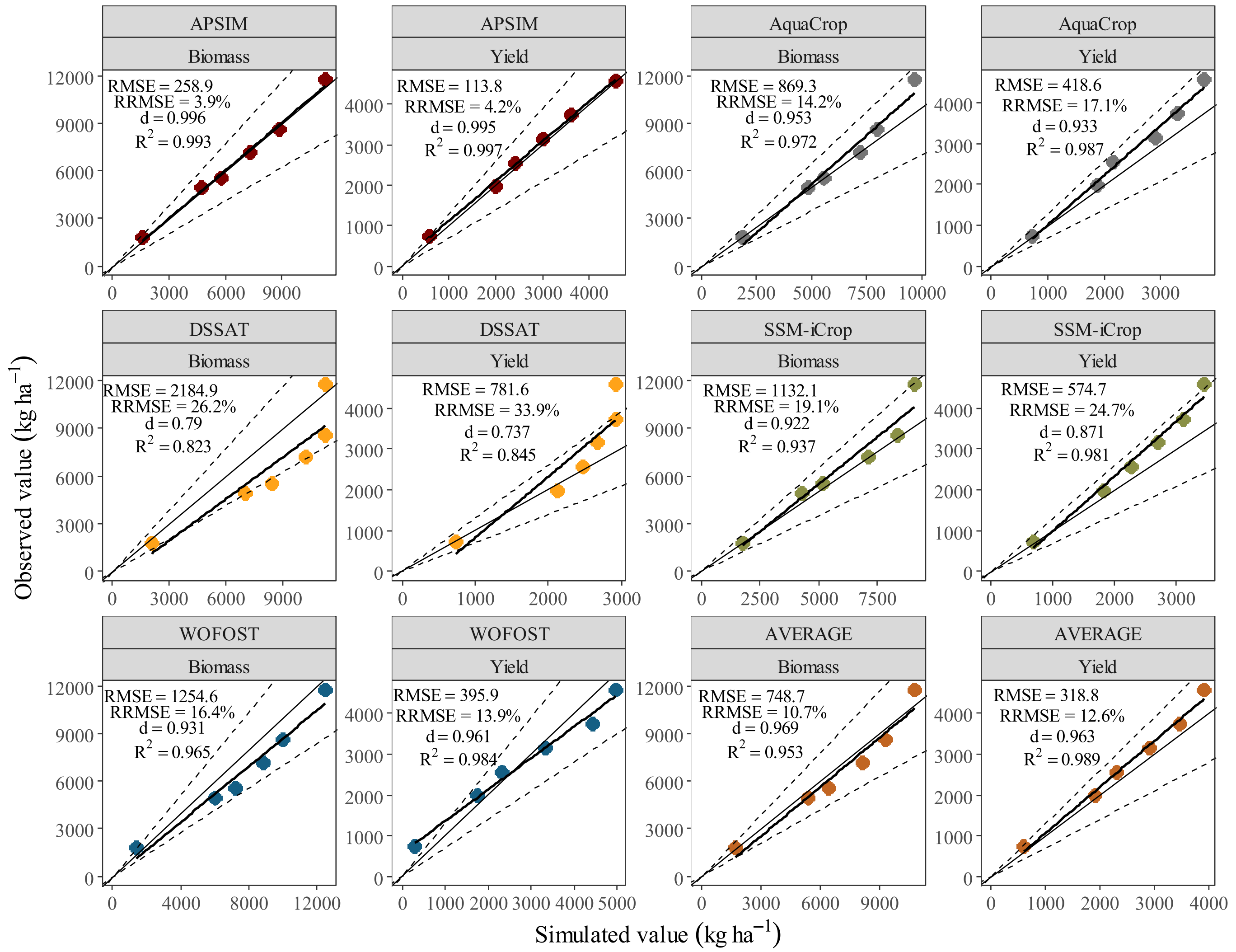

Fig. 8. Simulated versus measured aboveground biomass at maturity and final grain yield for spring wheat under different water treatments by different crop models at Pengyang in 2016. AVERAGE indicates the ensemble value of the five different models.

overestimate yield to varying extents. In contrast, under climate pattern A, four models (excluding WOFOST and the ensemble) generally underestimated yield. For climate pattern C, the WOFOST model underestimated yield, whereas the APSIM and AquaCrop models overestimated it.

Further analysis showed that the RMSE values of simulated yields did not consistently correspond with the observed values across different climate patterns (Fig. 11). Among the five models, APSIM, AquaCrop, and the ensemble of all five models exhibited the highest RMSE values under climate patterns D and E. The DSSAT model showed the highest RMSE under patterns C and E, while the SSM-iCrop model had the highest RMSE in patterns A and E. In contrast, the WOFOST model produced the highest RMSE in climate pattern B.

The RRMSE values for yield simulations also varied across different climate patterns (Fig. 12). All five individual models, as well as the ensemble model, exhibited consistently lower RRMSE values under climate patterns A, B, and C. In contrast, under climate patterns D and E, RRMSE values were markedly higher, exceeding 30 % in all cases. These results indicated that the simulation performance of both individual models and the ensemble was relatively poor under the climatic conditions represented by patterns D and E.

The d and R^2 for yield showed no clear pattern of variation across different climate patterns, as not displayed in the graph. Furthermore, the RMSE and RRMSE for spring wheat aboveground biomass at maturity had similar results with yield (Fig. S5, S6).

4. Discussion and conclusions

4.1. The performance of crop models varies under different year patterns of climate

Although growing-season precipitation is a critical determinant of spring wheat yield, the adverse effects of atmospheric evaporative demand (expressed in terms of vapor pressure deficit or reference evapotranspiration) on the growth and development of spring wheat should not be overlooked. Elevated atmospheric evaporative demand can inhibit stomatal opening in plant leaves (Novick et al., 2016), impeding the assimilation process and resulting in reduced dry matter accumulation and ultimately lower wheat yields (Zhao et al., 2020). Hence, we proposed using the atmospheric moisture condition (the difference between precipitation and reference evapotranspiration) in current study to better represent the influence of key meteorological factors during the growing season on the final yield of spring wheat. Given that the calculation of growing season atmospheric moisture conditions was based on both precipitation and reference evapotranspiration, and that reference evapotranspiration was influenced by air temperature, vapor pressure deficit, radiation, and wind speed, these interdependencies were also reflected in the correlation analysis (Fig. S3). Therefore, we

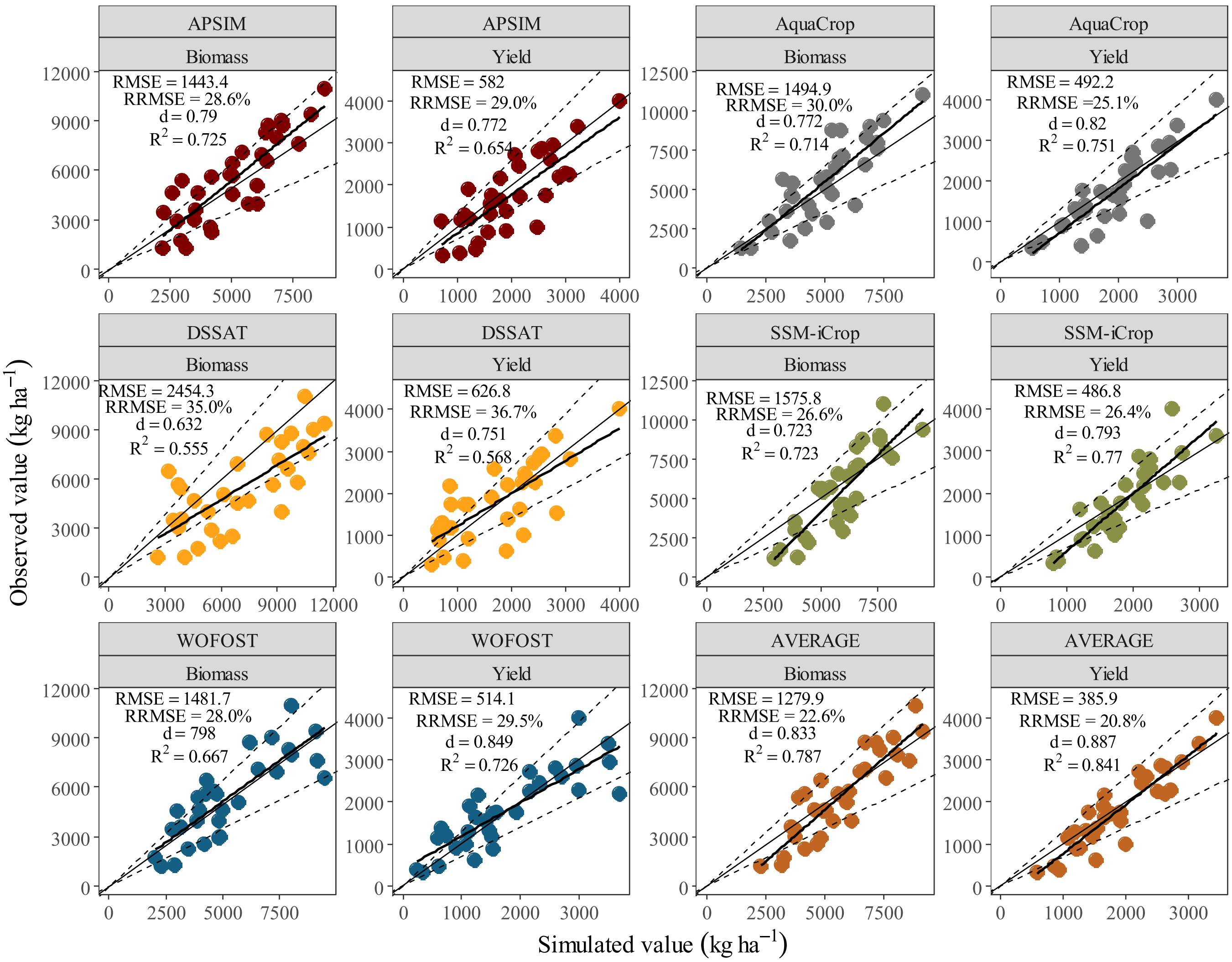

Fig. 9. Simulated versus measured aboveground biomass at maturity and final grain yield by different crop models during 1987–2018 in Dingxi. AVERAGE indicates the ensemble value of the five different models.

considered atmospheric moisture conditions to serve as an integrative indicator, effectively capturing the combined influence of these environmental variables on spring wheat yield.

In the study area, precipitation distribution exhibited poor synchronization with the phenological stages of spring wheat, particularly during the reproductive phase when precipitation was relatively scarce (monthly precipitation less than 100 mm, shown in Fig. 2). Consequently, soil water content at planting become a determinant factor influencing spring wheat growth and development (Fig. S2). From an agronomic perspective, soil water content at planting significantly affects two key physiological processes: 1) seedling establishment, suboptimal soil water conditions at planting directly impair germination rates and delay emergence timing (Fig. 4); 2) vegetative growth, adequate soil water storage at planting facilitates more efficient completion of the vegetative growth phase and promotes greater biomass accumulation, thereby enabling the crop to achieve optimal leaf area index (Li et al., 2004). When coupled with favorable atmospheric moisture conditions during reproductive growth, these factors collectively contributed to enhanced yield potential (Year pattern A in Fig. 5). Conversely, soil water deficit at planting restricted vegetative development, leading to suppressed biomass production and ultimately compromising final grain yield (Year pattern E in Fig. 5).

Previous studies have demonstrated that both the duration of the reproductive stage and initial soil moisture conditions are key determinants of crop final yield (Nielsen et al., 2010). Unlike other crops, spring wheat exhibits a comparatively shorter reproductive phase. Consequently, classifying climatic patterns based on soil water content at planting and atmospheric moisture conditions during the growing season provides a scientifically sound approach for analyzing spring wheat growth dynamics, developmental processes, and yield formation.

In current crop modeling practices, parameter calibration typically relies on data from years with sufficient water supply or specific experimental data from individual year. This approach often fails to account for how crops grow, develop, and form yields under extreme climate conditions or unusual weather events. While models can accurately simulate crop growth and yield under normal or specific conditions, this does not guarantee their accuracy in extreme years. Parameters calibrated for certain years or conditions may only work well for those same situations (Wallach and Thorburn, 2017). Under extreme conditions, such as drought or waterlogging, models may overestimate final crop yields (Hao et al., 2021; Li et al., 2019), as also shown in this study. In our analysis, five individual models and their ensemble struggled to correctly simulate spring wheat yield variations during droughts (e.g., extreme year type E). Additionally, from 1987 to 2018, four extreme dry years occurred (Fig. 13). Most models tend to ignore such unusual year patterns during calibration, leading to unavoidable yield prediction errors in these cases.

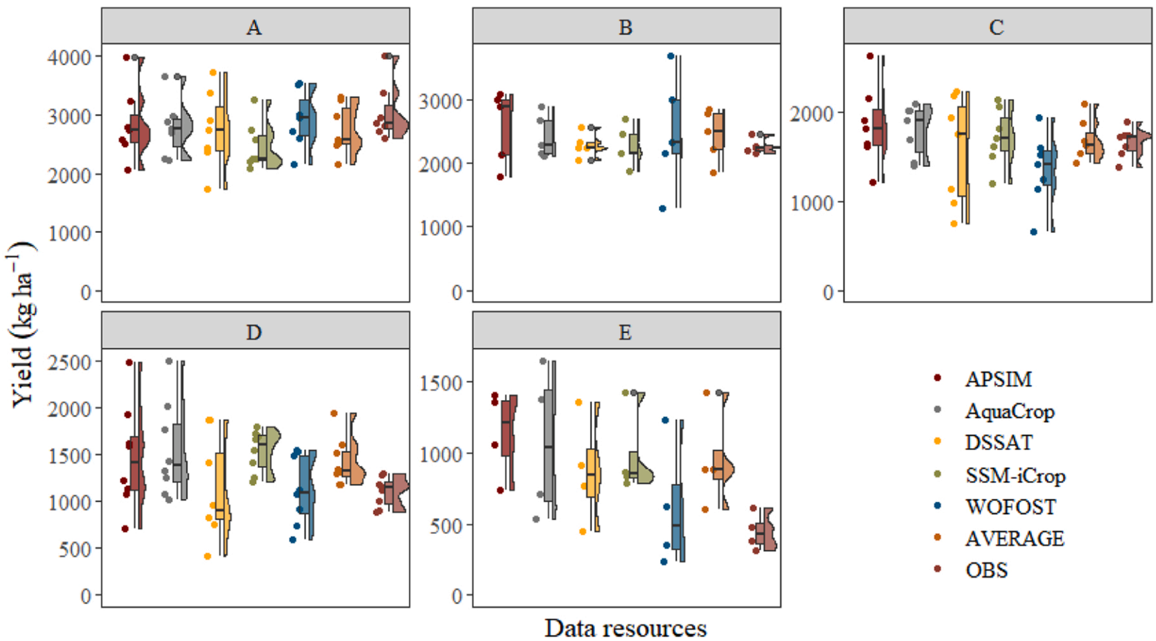

Fig. 10. Comparison of observed final grain yield and simulated final grain yield for spring wheat by different crop models under different year patterns of climate. AVERAGE indicates the ensemble value of the five different models.

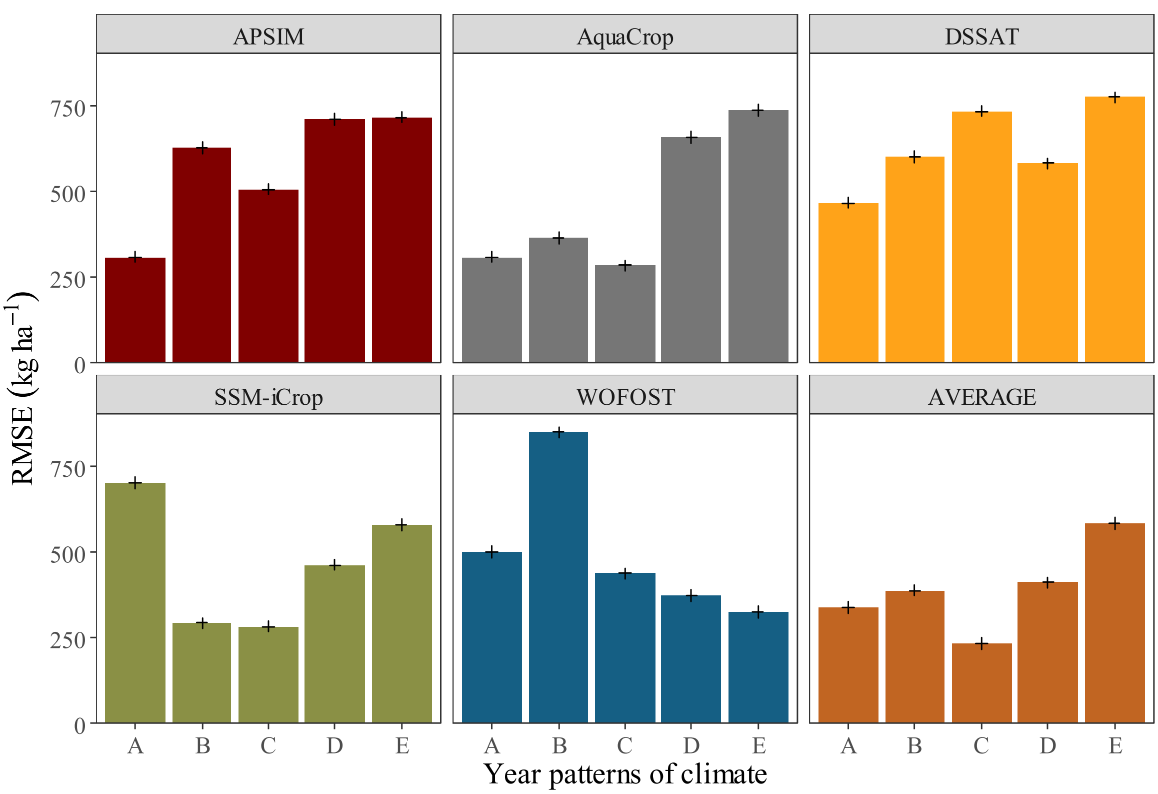

Fig. 11. Comparison of root mean square error (RMSE) between observed final grain yield and simulated final grain yield for spring wheat by different crop models under different year patterns of climate. AVERAGE indicates the ensemble value of the five different models.

For densely planted crops like wheat, key factors such as seeding density, emergence rate, emergence timing, and tillering significantly influence yield formation (Fig. 4). These factors can greatly affect model simulation accuracy. However, most crop models use a fixed, predefined sowing density. They focus mainly on how drought affects leaf growth and biomass accumulation, often overlooking its impact on emergence and tillering (Soltani and Sinclair, 2012). In practice, emergence and tillering depend heavily on soil moisture at planting, especially in water-limited areas (Lyon et al., 1995). As a result, models may produce inaccurate yield estimates in regions or studies where soil moisture at planting varies significantly.

As climate warming intensifies, atmospheric evaporative demand continues to rise globally (Novick et al., 2016). Changes in atmospheric moisture conditions at the daily scale affect crop photosynthetic

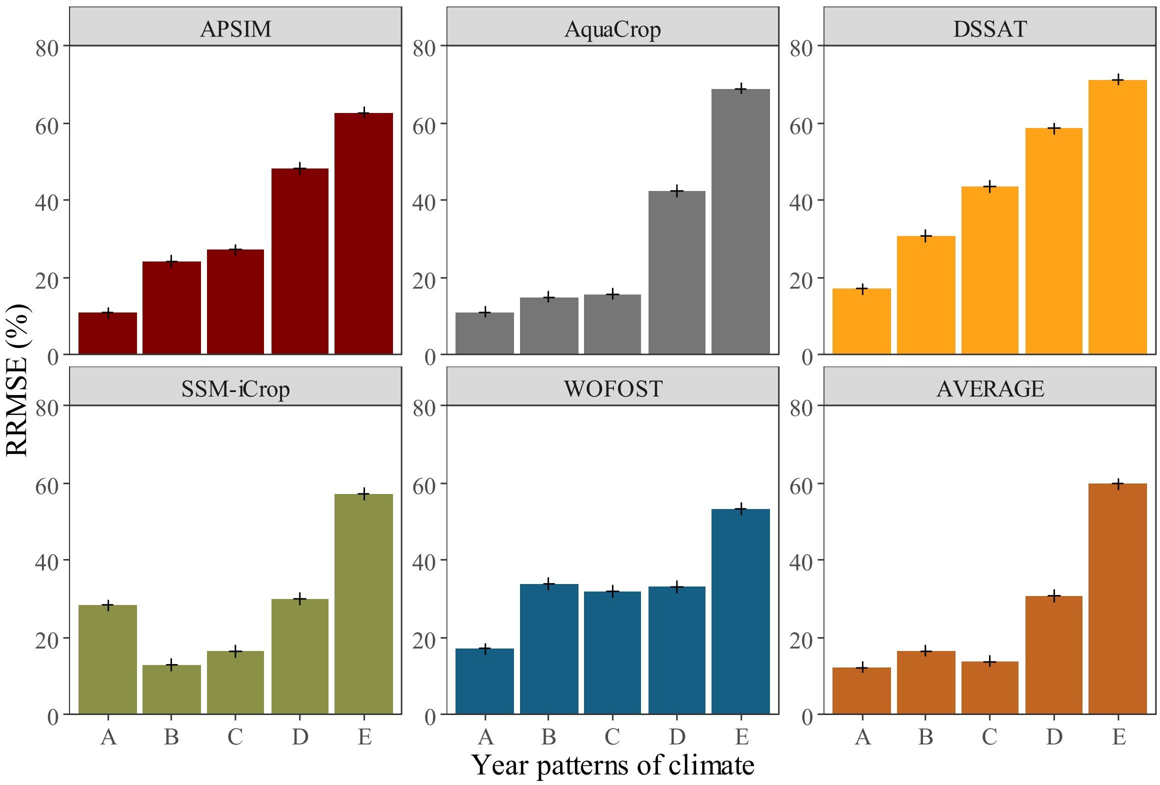

Fig. 12. Comparison of relative root mean square error (RRMSE) between observed final grain yield and simulated final grain yield for spring wheat by different crop models under different year patterns of climate. AVERAGE indicates the ensemble value of the five different models.

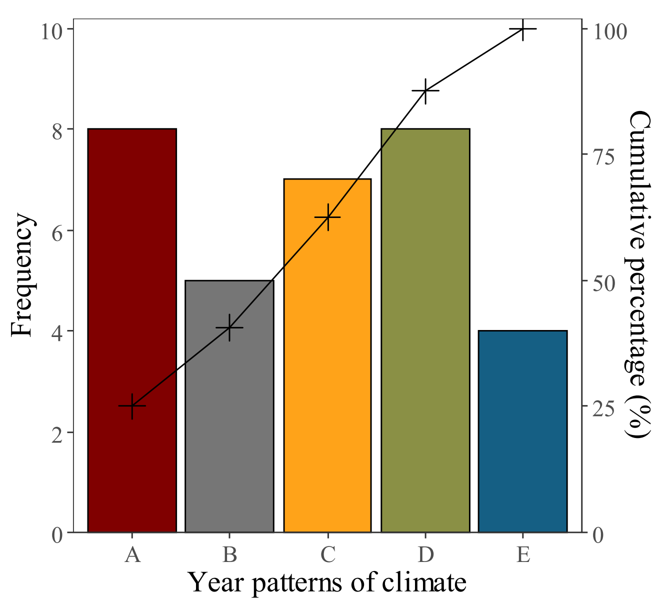

Fig. 13. Frequency and cumulative percentage of different year patterns of climate in Dingxi.

processes. Higher evaporative demand reduces stomatal conductance, leading to lower leaf assimilation rates and ultimately reduced carbon accumulation in crops (Rigden et al., 2020; Koehler et al., 2023). However, most current crop models are based on light-use efficiency and inadequately account for how atmospheric dryness influences crop growth and yield formation (Nóia Júnior et al., 2025). As a result, they struggle to accurately simulate yield reductions due to underestimation of crop water use under increasing evaporative demand (Webber et al., 2025). This is also one reason why, in this study, the crop models performed less accurately in drier growing seasons (Year patterns D and E in current study).

Some studies suggest that crop models tend to underestimate yields when low rainfall limits growing-season productivity (Yu et al., 2014), a finding that contrasts with our results. However, most research agrees that models typically overestimate yields during droughts (Hao et al., 2021), which aligns with our conclusions. In fact, whether crop models overestimate or underestimate crop yield may depend on the severity of the drought stress experienced by the crops. In extreme drought conditions, crop growth and yield are often limited by multiple factors, not just water scarcity. Temperature, light intensity, and air humidity may also shift from optimal to stressful conditions under drought (as crops become more sensitive to environmental stresses) (Farooq et al., 2009). These coupled stresses further restrict crop development and productivity. However, most crop models fail to account for these interacting stress factors (Nóia Júnior et al., 2025). As a result, they might tend to overestimate crop yields. In contrast, under mild or moderate drought conditions, crops may not necessarily experience yield loss as soon as drought occurs. Due to their adaptive strategies, crops might even exhibit compensatory growth if water supply improves later in the growing season (Farooq et al., 2009). However, since crop models cannot fully simulate these adaptive mechanisms, they may underestimate crop yields in such cases.

4.2. Implication for application of crop model under different conditions

Crop models are regularly adjusted and checked using experimental data collected over several years (Wallach et al., 2017). However, we often cannot fully trust the model results. This is mainly because the process of setting up and testing these models doesn't include enough different weather conditions that we know can happen based on long-term weather records (Yu et al., 2014). One of the biggest problems in crop modeling is that we usually don't have enough data covering several decades. This makes it hard to include all possible weather patterns that might occur in a specific area. While it's not realistic to adjust and test crop models for every possible weather situation, we also need to recognize that these models may not work well when applied to climate conditions they weren't tested for. The inherent limitations of crop models introduce uncertainty when applying them to real-world situations.

This research specifically examines wheat yield formation modeling across different annual climate patterns. However, we must consider the implications of substituting temporal data for spatial analysis. Our findings suggest that model performance may vary significantly across different locations, even within relatively close geographical areas. For example, when a model is calibrated for one particular region, applying it to nearby but drier areas could result in inaccurate crop growth and yield estimates. This occurs despite the close physical proximity between these locations. Such limitations can substantially impact the reliability and practical usefulness of model simulations.

When using crop models in water-limited conditions, it is crucial to recognize their potential uncertainty and tendency to overestimate yields. Typically, researchers validate these models against real-world field data to ensure reliability before applying them to climate change projections for food production forecasting. However, future climate scenarios indicate increasing drought frequency and severity, alongside declining water availability for rain-fed agriculture (Santini et al., 2022). Under these conditions, crop models may systematically underestimate yield losses. Our findings highlight the need to incorporate greater prediction uncertainty when using dynamic mathematical models to evaluate future food production and security.

CRediT authorship contribution statement

Heling Wang: Writing – review & editing, Validation, Investigation. **Qiang Zhang:** Supervision, Resources, Conceptualization. **Kai Zhang:** Writing – original draft, Visualization, Formal analysis, Data curation. **Funian Zhao:** Writing – original draft, Software, Methodology, Formal analysis, Conceptualization.

Declaration of Competing Interest

The authors declare that they have no known competing financial interests or personal relationships that could have appeared to influence the work reported in this paper.

Acknowledgements

The authors sincerely thank the anonymous reviewers for their valuable comments and suggestions for improving the quality of this paper. This work was jointly supported by Gansu Provincial Key Science and Technology Special Projects (25ZDFA011), National Natural Science Foundation of China (42230611, 42361060), Research Project of Arid Meteorological Science (IAM202420), Natural Science Foundation of Gansu Province (25JRRA353), and Central Guidance on Local Science and Technology Development Fund of Gansu Province (25ZYJA035).

Appendix A. Supporting information

Supplementary data associated with this article can be found in the online version at doi:10.1016/j.agwat.2025.109704.

Data availability

Data will be made available on request.

References

Allen, R., Pereira, L., Raes, D., Smith, M., 1998. FAO irrigation and drainage paper No. 56. Rome Food Agric. Organ. U. Nations 56, 26–40.

Balwinder-Singh, Gaydon, D.S., Humphreys, E., Eberbach, P.L., 2011. The effects of mulch and irrigation management on wheat in Punjab, India—evaluation of the APSIM model. Field Crops Res. 124, 1–13. https://doi.org/10.1016/j.fcr.2011.04.016.

Correndo, A., Rosso, L., Hernandez, C., Bastos, L., Nieto, L., Holzworth, D., Ciampitti, I., 2022. metrica: an R package to evaluate prediction performance of regression and classification point-forecast models. J. Open Source Softw. 7, 4655. https://doi.org/10.21105/joss.04655.

Farooq, M., Wahid, A., Kobayashi, N., Fujita, D., Basra, S.M.A., 2009. Plant drought stress: effects, mechanisms and management. Agron. Sustain. Dev. 29, 185–212. https://doi.org/10.1051/agro:2008021.

Fletcher, A.L., Chen, C., Ota, N., Lawes, R.A., Oliver, Y.M., 2020. Has historic climate change affected the spatial distribution of water-limited wheat yield across Western Australia? Clim. Change 159, 347–364. https://doi.org/10.1007/s10584-020-02666-w.

Hajjarpoor, A., Nelson, W.C.D., Vadez, V., 2022. How process-based modeling can help plant breeding deal with G x E x M interactions. Field Crops Res. 283, 108554. https://doi.org/10.1016/j.fcr.2022.108554.

Hao, S., Ryu, D., Western, A., Perry, E., Bogena, H., Franssen, H.J.H., 2021. Performance of a wheat yield prediction model and factors influencing the performance: a review and meta-analysis. Agric. Syst. 194, 103278. https://doi.org/10.1016/j.agsy.2021.103278.

Jin, Z., Zhuang, Q., Tan, Z., Dukes, J.S., Zheng, B., Melillo, J.M., 2016. Do maize models capture the impacts of heat and drought stresses on yield? Using algorithm ensembles to identify successful approaches. Glob. Chang Biol. 22, 3112–3126. https://doi.org/10.1111/gcb.13376.

Jones, J.W., Antle, J.M., Basso, B., Boote, K.J., Conant, R.T., Foster, I., Godfray, H.C.J., Herrero, M., Howitt, R.E., Janssen, S., Keating, B.A., Munoz-Carpena, R., Porter, C. H., Rosenzweig, C., Wheeler, T.R., 2017. Brief history of agricultural systems modeling. Agric. Syst. 155, 240–254. https://doi.org/10.1016/j.agsy.2016.05.014.

Jones, J.W., Hoogenboom, G., Porter, C.H., Boote, K.J., Batchelor, W.D., Hunt, L.A., Wilkens, P.W., Singh, U., Gijsman, A.J., Ritchie, J.T.2003. The DSSAT cropping system model. European Journal of Agronomy, Modelling Cropping Systems: Science, Software and Applications 18, 235–265. https://doi.org/10.1016/S1161-0301(02)00107-7.

Keating, B.A., Carberry, P.S., Hammer, G.L., Probert, M.E., Robertson, M.J., Holzworth, D., Huth, N.I., Hargreaves, J.N.G., Meinke, H., Hochman, Z., McLean, G., Verburg, K., Snow, V., Dimes, J.P., Silburn, M., Wang, E., Brown, S., Bristow, K.L., Asseng, S., Chapman, S., McCown, R.L., Freebairn, D.M., Smith, C.J.2003. An overview of APSIM, a model designed for farming systems simulation. European Journal of Agronomy, Modelling Cropping Systems: Science, Software and Applications 18, 267–288. https://doi.org/10.1016/S1161-0301(02)00108-9.

Kleinwechter, U., Gastelo, M., Ritchie, J., Nelson, G., Asseng, S., 2016. Simulating cultivar variations in potato yields for contrasting environments. Agric. Syst. 145, 51–63. https://doi.org/10.1016/j.agsy.2016.02.011.

Koehler, T., Wankmüller, F.J.P., Sadok, W., Carminati, A., 2023. Transpiration response to soil drying versus increasing vapor pressure deficit in crops: physical and physiological mechanisms and key plant traits. J. Exp. Bot. 74, 4789–4807. https://doi.org/10.1093/jxb/erad221.

Li, Y., Guan, K., Schnitkey, G.D., DeLucia, E., Peng, B., 2019. Excessive rainfall leads to maize yield loss of a comparable magnitude to extreme drought in the United States. Glob. Chang Biol. 25, 2325–2337. https://doi.org/10.1111/gcb.14628.

Li, F.-M., Wang, P., Wang, J., Xu, J.-Z., 2004. Effects of irrigation before sowing and plastic film mulching on yield and water uptake of spring wheat in semiarid Loess Plateau of China. Agric. Water Manag. 67, 77–88. https://doi.org/10.1016/j.agwat.2004.02.001.

Li, Y., Zhang, S., Liu, Q., Ji, Y., Yao, N., Song, X., 2021. Effects of droughts and meteorology on spring wheat in western loess plateau based on DSSAT-CERES-wheat model. Trans. Chin. Soc. Agric. Mach. 53, 338–348. https://doi.org/10.6041/j.issn.1000-1298.2022.06.036.

Lyon, D.J., Boa, F., Arkebauer, T.J., 1995. Water-yield relations of several spring-planted dryland crops following winter wheat. J. Prod. Agric. 8, 281–286. https://doi.org/10.2134/jpa1995.0281.

Manschadi, A.M., Eitzinger, J., Breisch, M., Fuchs, W., Neubauer, Soltani, A., 2020. Full parameterisation matters for the best performance of crop models: inter-comparison of a simple and a detailed maize model. Int. J. Plant Prod. 15. https://doi.org/10.1007/s42106-020-00116-2.

Nie, Z., Li, G., Luo, C., Ma, W., Dai, Y., 2018. Parameter optimization in APSIM-based simulation model for yield formation of dryland wheat using shuffled frog leaping algorithm. Acta Agron. Sin. 44, 1229–1236. https://doi.org/10.3724/SP.J.1006.2018.01229.

Nielsen, D.C., Halvorson, A.D., Vigil, M.F., 2010. Critical precipitation period for dryland maize production. Field Crops Res. 118, 259–263. https://doi.org/10.1016/j.fcr.2010.06.004.

Nóia Júnior, R. de S., Asseng, S., Müller, C., Deswarte, J.-C., Cohan, J.-P., Martre, P., 2025. Negative impacts of climate change on crop yields are underestimated. Trends Plant Sci. https://doi.org/10.1016/j.tplants.2025.05.002. S13601385(25)00130X.

Novick, K.A., Ficklin, D.L., Stoy, P.C., Williams, C.A., Bohrer, G., Oishi, A.C., Papuga, S. A., Blanken, P.D., Noormets, A., Sulman, B.N., Scott, R.L., Wang, L., Phillips, R.P., 2016. The increasing importance of atmospheric demand for ecosystem water and carbon fluxes. Nat. Clim. Change 6, 1023–1027. https://doi.org/10.1038/nclimate3114.

Otkin, J.A., Svoboda, M., Hunt, E.D., Ford, T.W., Anderson, M.C., Hain, C., Basara, J.B., 2018. Flash Droughts: A Review and Assessment of the Challenges Imposed by Rapid-Onset Droughts in the United States. Bull. Am. Meteorol. Soc. 99, 911–919. https://doi.org/10.1175/BAMS-D-17-0149.1.

Palosuo, T., Kersebaum, K.C., Angulo, C., Hlavinka, P., Moriondo, M., Olesen, J.E., Patil, R.H., Ruget, F., Rumbaur, C., Takáč, J., Trnka, M., Bindi, M., Çaldağ, B., Ewert, F., Ferrise, R., Mirschel, W., Şaylan, L., Šiška, B., Rötter, R., 2011. Simulation of winter wheat yield and its variability in different climates of Europe: A comparison of eight crop growth models. Eur. J. Agron. 35, 103–114. https://doi.org/10.1016/j.eja.2011.05.001.

R Development Core Team, 2024. R: A language and environment for statistical computing. MSOR connections.

Ramirez-Villegas, J., Koehler, A.-K., Challinor, A.J., 2017. Assessing uncertainty and complexity in regional-scale crop model simulations. Eur. J. Agron. Uncertain. Crop Model Predict. 88, 84–95. https://doi.org/10.1016/j.eja.2015.11.021.

Rigden, A.J., Mueller, N.D., Holbrook, N.M., Pillai, N., Huybers, P., 2020. Combined influence of soil moisture and atmospheric evaporative demand is important for accurately predicting US maize yields. Nat. Food 1, 127–133. https://doi.org/10.1038/s43016-020-0028-7.

Santini, M., Noce, S., Antonelli, M., Caporaso, L., 2022. Complex drought patterns robustly explain global yield loss for major crops. Sci. Rep. 12, 5792. https://doi.org/10.1038/s41598-022-09611-0.

Sinclair, T.R., 1986. Water and nitrogen limitations in soybean grain production I. Model development. Field Crops Res. 15, 125–141. https://doi.org/10.1016/0378-4290(86)90082-1.

Soltani, A., Alimagham, S.M., Nehbandani, A., Torabi, B., Zeinali, E., Dadrasi, A., Zand, E., Ghassemi, S., Pourshirazi, S., Alasti, O., Hosseini, R.S., Zahed, M., Arabameri, R., Mohammadzadeh, Z., Rahban, S., Kamari, H., Fayazi, H., Mohammadi, S., Keramat, S., Vadez, V., van Ittersum, M.K., Sinclair, T.R., 2020. SSM-iCrop2: a simple model for diverse crop species over large areas. Agric. Syst. 182, 102855. https://doi.org/10.1016/j.agsy.2020.102855.

Soltani, A., Sinclair, T.R., 2012. Modeling physiology of crop development, growth and yield. Model. Physiol. Crop Dev. Growth yield 1–322.

Soltani, A., Sinclair, T.R., 2015. A comparison of four wheat models with respect to robustness and transparency: Simulation in a temperate, sub-humid environment. Field Crops Res. 175, 37–46. https://doi.org/10.1016/j.fcr.2014.10.019.

Steduto, P., Hsiao, T.C., Raes, D., Fereres, E., 2009. AquaCrop—The FAO crop model to simulate yield response to water: I. Concepts and underlying principles. Agron. J. 101, 426–437. https://doi.org/10.2134/agronj2008.0139s.

Teixeira, E.I., Zhao, G., Ruiter, J. de, Brown, H., Ausseil, A.-G., Meenken, E., Ewert, F., 2017. The interactions between genotype, management and environment in regional crop modelling. Eur. J. Agron. Uncertain. Crop Model Predict. 88, 106–115. https://doi.org/10.1016/j.eja.2016.05.005.

Wallach, D., Nissanka, S.P., Karunaratne, A.S., Weerakoon, W.M.W., Thorburn, P.J., Boote, K.J., Jones, J.W., 2017. Accounting for both parameter and model structure uncertainty in crop model predictions of phenology: a case study on rice. Eur. J. Agron. Uncertain. Crop Model Predict. 88, 53–62. https://doi.org/10.1016/j.eja.2016.05.013.

Wallach, D., Thorburn, P.J., 2017. Estimating uncertainty in crop model predictions: Current situation and future prospects. Eur. J. Agron. Uncertain. Crop Model Predict. 88, A1–A7. https://doi.org/10.1016/j.eja.2017.06.001.

Webber, H., Cooke, D., Wang, C., Asseng, S., Martre, P., Ewert, F., Kimball, B., Hoogenboom, G., Evett, S., Chanzy, A., Garrigues, S., Olioso, A., Copeland, K.S., Steiner, J.L., Cammarano, D., Chen, Y., Crépeau, M., Diamantopoulos, E., Ferrise, R., Manceau, L., Gaiser, T., Gao, Y., Gayler, S., Guarin, J.R., Hunt, T., Jégo, G., Padovan, G., Pattey, E., Ripoche, D., Rodríguez, A., Ruiz-Ramos, M., Shelia, V., Srivastava, A.K., Supit, I., Tao, F., Thorp, K., Viswanathan, M., Weber, T., White, J., 2025. Wheat crop models underestimate drought stress in semi-arid and Mediterranean environments. Field Crops Res. 332, 110032. https://doi.org/10.1016/j.fcr.2025.110032.

White, K.E., Fleisher, D.H., Cavigelli, M.A., Timlin, D.J., Schomberg, H.H., 2025. Assessing long-term weather variability impacts on annual grain yields using a maize simulation model. Agric. For. Meteorol. 370, 110593. https://doi.org/10.1016/j.agrformet.2025.110593.

de Wit, A., Boogaard, H., Fumagalli, D., Janssen, S., Knapen, R., van Kraalingen, D., Supit, I., van der Wijngaart, R., van Diepen, K., 2019. 25 years of the WOFOST cropping systems model. Agric. Syst. 168, 154–167. https://doi.org/10.1016/j.agsy.2018.06.018.

Yu, Q., Li, L., Luo, Q., Eamus, D., Xu, S., Chen, C., Wang, E., Liu, J., Nielsen, D.C., 2014. Year patterns of climate impact on wheat yields. Int. J. Climatol. 34, 518–528. https://doi.org/10.1002/joc.3704.

Zhang, K., Li, Q., Wang, R., Guo, L., Lei, J., Yao, Y., Wang, H., 2012. Effects of sowing date on the growth and yield of spring wheat. Chin. J. Ecol. 31, 324.

Zhang, Q., Yang, Z., Hao, X., Yue, P., 2019. Conversion features of evapotranspiration responding to climate warming in transitional climate regions in northern China. Clim. Dyn. 52, 3891–3903. https://doi.org/10.1007/s00382-018-4364-3.

Zhao, F., Lei, J., Wang, R., Wang, H., Zhang, K., Yu, Q., 2018. Determining agricultural drought for spring wheat with statistical models in a semi-arid climate. J. Agric. Meteor. 74, 162–172. https://doi.org/10.2480/agrmet.D-18-00011.

Zhao, F., Lei, J., Wang, R., Zhang, Q., Qi, Y., Zhang, K., Guo, Q., Wang, H., 2022. Environmental determination of spring wheat yield in a climatic transition zone under global warming. Int. J. Biometeorol. 66, 481–491. https://doi.org/10.1007/s00484-021-02196-9.

Zhao, F., WANG, R., Zhang, K., LEI, J., Yu, Q., 2019. Predicting spring wheat yields based on water use-yield production function in a semi-arid climate. Span. J. Agric. Res. 17, e1201. https://doi.org/10.5424/sjar/2019172-14699.

Zhao, F., Zhang, Q., Lei, J., Wang, H., Zhang, K., Qi, Y., 2024. Environmental factors influence the responsiveness of potato tuber yield to growing season precipitation. Crop Environ. https://doi.org/10.1016/j.crope.2024.02.002.

Zhao, F., Zhou, S., Wang, R., Zhang, K., Wang, H., Yu, Q., 2020. Quantifying key model parameters for wheat leaf gas exchange under different environmental conditions. J. Integr. Agric. 19, 2188–2205. https://doi.org/10.1016/S2095-3119(19)62796-6.